New photocatalysts based on mixed-metal pyridine dicarboxylates

Partha Mahata,[a] Giridhar Madras,[b,*] and Srinivasan Natarajan[a,*]

[a]*Framework Solids Laboratory, Solid State and Structural Chemistry Unit, Indian Institute of Science, Bangalore 560 012, India*
[b]*Department of Chemical Engineering, Indian Institute of Science, Bangalore 560 012, India*

New photocatalytically active isostructural two-dimensional mixed metal-pyridine dicarboxylates, $[M(H_2O)_3Co\{C_5N_1H_3(COO)_2\}_3])_\infty]$, M = Gd (**1**), Dy (**2**) and Y (**3**) have been prepared under hydrothermal conditions. The structure consists of a network of $MO_6(H_2O)_3$, CoO_3N_3 polyhedral units connected by the pyridine dicarboxylates forming two-dimensional layers, which are arranged in an *AAAA*... fashion. The photocatalytic studies on **1** – **3** indicate that they are active catalysts for the degradation of simple organic dyes, such as Remazol brilliant blue R (RBBR) and Orange G (OG) in the presence of UV light. The compounds have also been characterized by powder XRD, IR, TGA, UV-Vis and magnetic studies.

KEY WORDS: photocatalysts; hydrothermal conditions; mixed-metal carboxylates; UV light; organic dyes.

1. Introduction

Heterogeneous catalysis is an important area of study requiring development of new functional catalysts for many important processes [1,2]. Photocatalysis is being used for the green ecological elimination of organic compounds or harmful pollutants [3–5]. It is also attracting increasing attention as a potentially clean and renewable source for hydrogen fuel by the splitting of water into H_2 and O_2 by means of solar-to-chemical conversion [6–10]. The solid photocatalysts commonly employed are semiconductor metal oxide and sulphide particles such as TiO_2, ZnO, WO_3, CdS, ZnS, and Fe_2O_3; layered niobates and titanates; and polyoxometallates (POM), mainly of W [3–5,11,12]. On the other hand, it is also important to search for new materials with improved photocatalytic properties. In this context, the photocatalytic studies of mixed-metal (*d*–*f*) hybrid compounds are just beginning to emerge [13,14]. The synthesis of such mixed-metal systems pose some difficulty for the following reasons: (a) the high coordination and low stereochemical preferences of the lanthanides, which limit their selective introduction into a highly ordered structure and (b) competitive reactions between 3*d* and 4*f* metals bonding to the same ligand, which often results in homometallic compounds rather than a hetero-metallic ones. Heterogeneous catalysis based on mixed-metals anchored on mesoporous silica has been well established [15,16].

We have undertaken a study of mixed-metal coordination compounds to explore and prepare new compounds with novel properties. During the course of these investigations, we have isolated a new mixed-metal coordination compounds of the general formula, $[M(H_2O)_3Co\{C_5N_1H_3(COO)_2\}_3])_\infty]$, M = Gd (**1**), Dy (**2**) and Y (**3**). The structure consist of a network $MO_6(H_2O)_3$ and Co_3N_3 polyhedral units, connected by the carboxylates anions. The photocatalytic studies, performed at room temperature, indicate the compounds to be active for the photodegradation of two commonly used organic dyes (Remazol brilliant blue R (RBBR) and Orange G (OG)) in textile industry. Despite similar band gap energies, the compounds are selective towards photodegradation. The synthesis, structure and preliminary studies on the Gd compound were reported earlier by us [17]. In this paper, we present a comprehensive investigation on the synthesis and photocatalytic studies of these compounds.

2. Experimental

All the compounds have been synthesized under similar conditions employing hydrothermal methods. In a typical synthesis, for **1**, 0.343 g of $Gd(NO_3)_3$, 0.252 g of $Co(OAc)_2 \cdot 4H_2O$ and 0.338 g of Pyridine-2,3-dicarboxylic acid were dissolved in 14 ml of water and the mixture was homogenized at room temperature for 30 min. The final reaction mixture with the composition, 1:1:2:780 was sealed in a 23 ml PTFE-lined stainless steel autoclave and heated at 140 °C for 72 h. The resulting product contained only dark pink rod like single crystals and was vacuum filtered and dried at ambient conditions. The yield of the product was ~70%. Identical composition and synthesis procedures were adapted for the preparation of the other two compounds, in very high yield (80%). We have also been

*To whom correspondence should be addressed.
  E-mails: giridhar@chemeng.iisc.ernet.in; snatarajan@sscu.iisc.ernet.in

able to prepare ~10 g batch samples by appropriate scaling of the reaction mixture.

The compounds were characterized by powder X-ray diffraction (XRD), IR spectroscopy, TGA, UV-visible spectroscopy. The powder XRD patterns were recorded on crushed single crystals in the 2θ range 5–50° using Cu-Kα radiation (Philips, X'pert-Pro). The observed XRD pattern matched very well with the XRD pattern simulated from the structure determined by single crystal X-ray diffraction.

Infrared (IR) spectroscopic studies have been carried in the mid-IR region on KBr pellets (Perkin–Elmer, SPEC-TRUM 1000). The IR spectra of all the compounds indicated characteristic sharp lines with very similar bands. Minor variations in the bands were, however, observed between the three compounds. The observed bands are: 3408(s)cm^{-1}–v_{as}OH, 2353(m) cm^{-1}–v_s(C–H)$_{aromatic}$, 1670(s) cm^{-1}–v_s(C=O), 1594(w) cm^{-1}–δ_sH$_2$O, 1561(m)–(C–C)$_{skeletal}$, 1331(s) cm^{-1}–δ_s(COO), 1275(m)cm^{-1}–δ(CH$_{aromatic}$)$_{in-of-plane}$, 1111(m) cm^{-1}–δ(C–N$_{skeletal}$), 880(w) cm^{-1}–δ(CH$_{aromatic}$)$_{out-of-plane}$.

Thermogravimetric analysis (TGA) has been carried out (Metler-Toledo) in flowing air (flow rate = 50 ml/min) in the temperature range 30–850 °C (heating rate = 5 °C/min). The results indicate all the three compounds behave in a similar fashion. An initial weight loss in the temperature 100–200 °C due to the loss of the bound water molecules and the second sharp weight loss in the temperature range 350–400 °C, corresponding with the loss of the carboxylate. The total observed weight loss of 72% (calc. 68%), 61% (calc. 67%) and 71 % (calc. 73%), respectively corresponds well with the loss of bound water molecules and the carboxylates.

2.1. Photocatalytic experiments

The photochemical reactor employed in this study comprised of a jacketed quartz tube of 3.4 cm inner diameter, 4 cm outer diameter, and 21 cm length and an outer Pyrex glass reactor of 5.7 cm id and 16 cm length. A high-pressure mercury vapor lamp (HPML) of 125 W (Philips, India) was placed inside the jacketed quartz tube after removal of the outer shell. The ballast and capacitor were connected in a series with the lamp to avoid the fluctuations in input supply. Water was circulated through the annulus of the quartz tube to avoid heating of the solution due to dissipative loss of UV energy. The solution was taken in the outer reactor and continuously stirred to ensure that the suspension of the catalyst was uniform. The lamp radiated predominantly at 365 nm corresponding to the energy of 3.4 eV and the photon flux is 5.8×10^{-6} mol of photons/s. Further details of the experimental setup can be found elsewhere [12].

For the degradation studies, the dyes were dissolved in double distilled Millipore filtered water. The effect of the initial concentration of the dyes and the effect of

catalyst loading on the reaction rates was investigated. The reactions were carried out at 40 °C, which was maintained by circulating water in annulus of the jacketed quartz reactor. Samples were collected at regular intervals, filtered through Millipore membrane filters, and centrifuged to remove the catalyst particles prior to analysis, as described below.

Samples were analyzed with a Perkin–Elmer UV-visible spectrophotometer (model Lambda 32). The calibration for RBBR and OG was based on Beer–Lambert law at its maximum absorption wavelength, λ_{max} of 590 and 482 nm, respectively.

3. Results and discussion

3.1. Structure

All the three compounds are isostructural and are formed by MO$_9$ tricapped trigonal prismatic units and Co$_3$N$_3$ octahedral units. The connectivity between these and the pyridine dicarboxylate anions give rise to a two-dimensional neutral layered structure. The detailed crystal structure description can be found elsewhere [17]. The layers are arranged in a *AAAA...* fashion, giving rise to a solid with a supermesh of apertures of ca 7 Å free diameter (figure 1).

3.2. UV-visible spectra

The room temperature diffuse reflectance UV-Vis spectra for the compounds **1, 2** and **3** indicate a main absorption band at 304 nm (figure 2). This band can be assigned to the ligand to metal charge transfer (LMCT). There are two other peaks, one at 381 nm and another one at 516 nm, which are due to the d-d transition of the Co^{+3} (d^6) ions. These two peaks can be assigned to the two spin allowed transitions, $^1A_{1g} \rightarrow {}^1T_{2g}$ and $^1A_{1g} \rightarrow {}^1T_{1g}$,
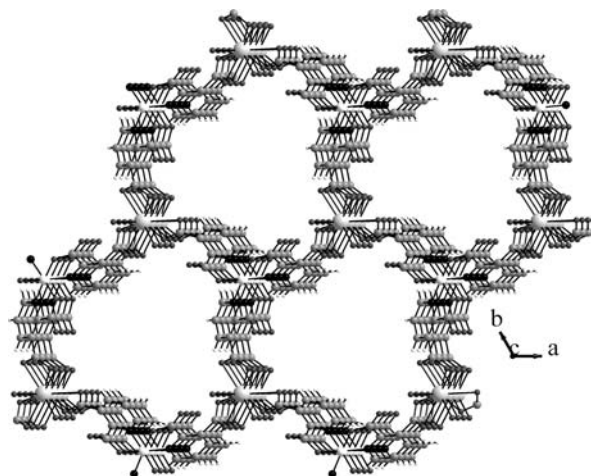

Figure 1. View of the structure of **1** showing the arrangement of the layers. Note that the layers are arranged in a *AAAA...* fashion giving rise to a one-dimensional channel (see text).
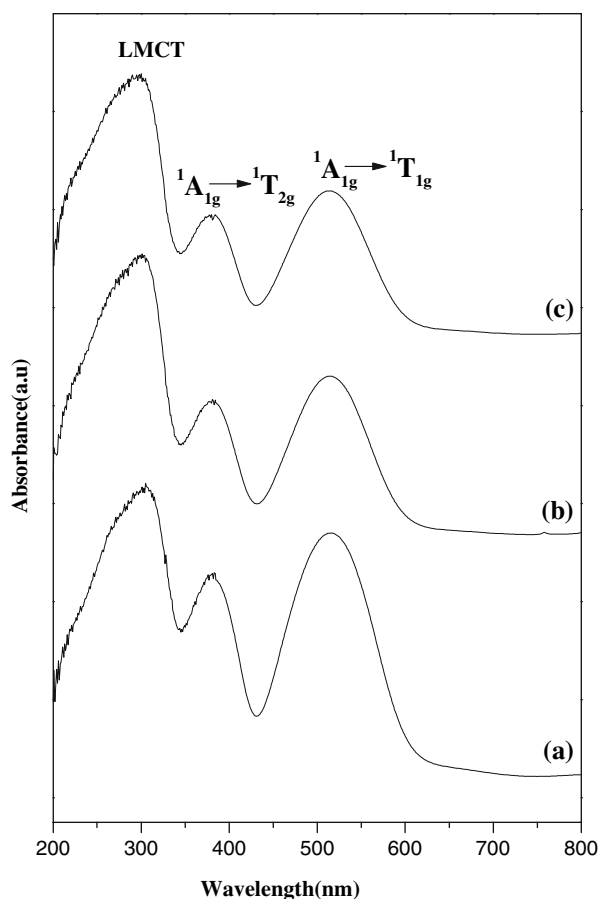
Figure 2. UV-visible spectra of $\{M(H_2O)_3Co[C_5N_1H_3(COO)_2]_3\}$: (a) M = Gd (**1**), (b) M = Dy (**2**) and (c) M = Y (**3**.)

respectively [18,19]. To obtain the precise values of band gap from the absorption edges, the point of inflection determined from the minimum in the first derivative of the absorption spectrum was used. The values of band gap, thus obtained, for all the three compounds correspond to ~3.7 eV.

3.3. Magnetic studies

The variable temperature magnetic susceptibility studies have been carried out on powdered samples using a SQUID magnetometer. The molar magnetic susceptibility (χ_M) increases with decreasing temperature. We did not observe any ordering in both the compounds. The plot of $1/\chi_M$ versus T plot clearly shows that both the compounds are paramagnetic in nature. The observed effective magnetic moment of **1** and **2** at room temperature were found to be 6.89 μ_B (calc 7.93) and 9.32μ_B (calc 10.63) [18,20], respectively. It is likely that the predominant contribution to the magnetic moment would be due to the M^{+3} ions (Gd or Dy) as the Co^{+3} ions appear to be in the low-spin state, (t_{2g}^6, e_g^0). Both **1** and **2**, show a small difference in the observed and calculated magnetic moment, which may be due to the presence of the diamagnetic Co^{+3} ions.

Additionally, in **2** there could be some contribution from the orbital quenching in the presence of the ligand field, though such effects for the f electron systems are always very small. The magnetic behavior of **3** is quite different from **1** and **2**. At room temperature, it shows a diamagnetic behavior, because Y^{+3} ions do not have any free electrons and Co^{+3} ions exist in low-spin.

3.4. Photocatalytic investigations

The photocatalytic degradation of two commonly used dyes, RBBR and OG, was investigated. We have selected these two dyes as model textile organic pollutants in aqueous media to demonstrate the efficacies of the photocatalytic behavior of the three compounds. The photocatalytic performance of the three compounds was estimated from the variation of the color in the reaction system by monitoring the absorbance (at λ_{max} = 590 and 482 nm) characteristic of the target RBBR and OG, which directly relate to the structural changes of their chromophore. For comparison, the photocatalytic performance of commercial TiO_2 (Degussa P-25) was also assessed under the same experimental conditions. Control experiments without the catalyst were also carried out and no degradation was observed. All the three compounds show good photocatalytic activity for the decomposition of RBBR and OG. The degradation profiles of RBBR and OG with an initial concentration of 100 ppm for different concentration of **1** varying from 0.5 kg/m^3 to 4 kg/m^3 are shown in figure 3(a) and (b), respectively. The variation of the initial rate with the loading of **1** for the degradation of RBBR and OG is shown as an inset of figure 3(a) and (b), respectively. The degradation of both the dyes is faster in presence of 1 g/L of **I** compared to that with same concentration Degussa P-25. As can be noted, the initial rate of degradation increases with an increase in the concentration of catalysts, but appears to saturate at a catalyst loading of 2 kg/m^3. This loading of the catalyst was used to investigate the degradation of RBBR and OG of different concentrations for all the three compounds. In order to quantify the reactions, the kinetics can be determined by the Langmuir-Hinshelwood (L-H) kinetics. This can be written as $r_0 = k_0C_0/(1 + K_0C_0)$, where r_0 is the initial rate, C_0 is the initial concentration of the dyes, k_0 is the kinetic rate constant and parameter K_0 represent the equivalent adsorption coefficient. The plot of the reciprocal initial degradation rate ($1/r_o$) with the reciprocal of the initial dye concentration (RBBR and OG) in presence of **1**, **2** and **3** is shown in figure 4(a), (b), repectively. The parameters, k_0, K_0, for the photocatalytic degradation of the dyes are obtained from the slope and the intercept of the linear plot. The values of k_0 and K_0 for the degradation of both the dyes by all three compounds are shown in Table 1.
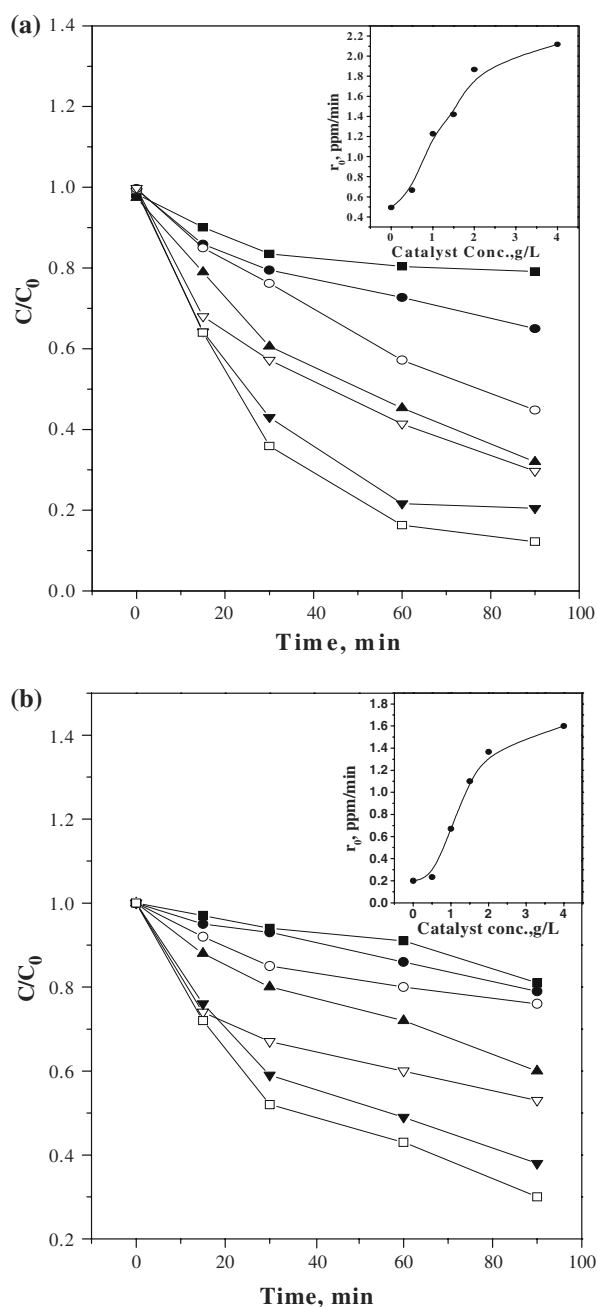
Figure 3. Degradation profiles for 100 ppm RBBR (a) or OG (b) without **1** (■), with 0.5 g/L (●), 1 g/L (▲), 1.5 g/L (▽), 2 g/L (▼), 4 g/L of I (□), with 1 g/L of Degussa P-25 (○). Inset shows the variation of the degradation rate with the catalyst concentration.

As the parameter, K_0, represents the adsorption equilibrium coefficient, the low value of K_0 can be attributed to negligible adsorption. This is also confirmed by powder XRD of the catalyst after the photocatalytic degradation experiments, which clearly indicated that the structure remained the same. For degradation of RBBR the rate coefficient k_0, varies in the order, **3** > **1** > **2** but for the degradation of OG, the order is **1** > **2** > **3**. It is clear that inspite of having comparable band gaps, the degradation rate of all the dyes are different and the order of the rate of degradation also appear to depend on the compound. This could probably be due to the selectivity of a particular compound to a particular dye. For example, OG is an azo dye and **1** might preferentially degrade azo dyes. To validate this hypothesis, the degradation of 100 ppm of two azo dyes (methyl red and methyl orange) was investigated using all the three compounds. The degradation rate of these dyes followed the order: **1** > **2** > **3**, the same as that obtained for the degradation of OG, confirming the selectivity of **1** for the azo dyes. These experiments also indicate that the synthesized compounds are not only photocatalytically active but also selective towards the degradation of specific organic functional groups.

The photocatalytic activity of the present compounds can be explained based on some of the earlier observations. The use of cobalt molecular complexes in the selective homogeneous photocatalytic cleavage of DNA has been known [21–25]. According to these studies, the low-spin Co^{3+} complexes, in general, show several types of excited states that include ligand-field (LF), intraligand (IL) and charge-transfer (CT) states. Of these, the IL and CT states are available and active due to the ligand π to metal empty e_g^* state, when nitrogen containing aromatic ligands are involved in bonding with the Co^{3+} [26]. Thus, the singlet or the triplet state of the aromatic ligand can, in principle, reduce the Co^{III} to Co^{II} and the radical cation that is formed during this reaction cleaves the DNA [22,23].

In the present compounds, we have a similar situation as cobalt exists in Co^{3+} and in low-spin state (empty e_g orbital). From our UV-Vis spectroscopic studies we clearly see three peaks, one belonging to the ligand-to-metal charge transfer effect (LMCT) and the other two belonging to the d–d spin allowed transitions. It is clear that the lanthanide ions in these compounds does not participate effectively in the electron transfer as the f orbitals are so well shielded from the surroundings of the ions, the various states arising from the f^n configurations are split by external fields only to the extent of ∼100 cm^{-1} [26]. The photocatalytic effect must have its origin from Co^{3+} ions, as it is rather difficult to ascertain precisely about the various electronic energy levels involved in these extended network compounds.

Although the photocatalytic experiments on **1**, **2** and **3** were carried out in heterogeneous conditions, it is believed that the photocatalytically active Co center would behave in a way similar to that in solution. Under these circumstances, we can adopt the mechanism employed to explain the DNA cleavage using low-spin Co^{+3} complexes in our present system. Of the three types of electronic states observed in the compounds, the LMCT effect, which is in the UV region, probably is responsible for the photocatalytic activity. Similar mechanism has been proposed recently for the degradation of organic dyes in the presence of 3d–5f mixed-metal
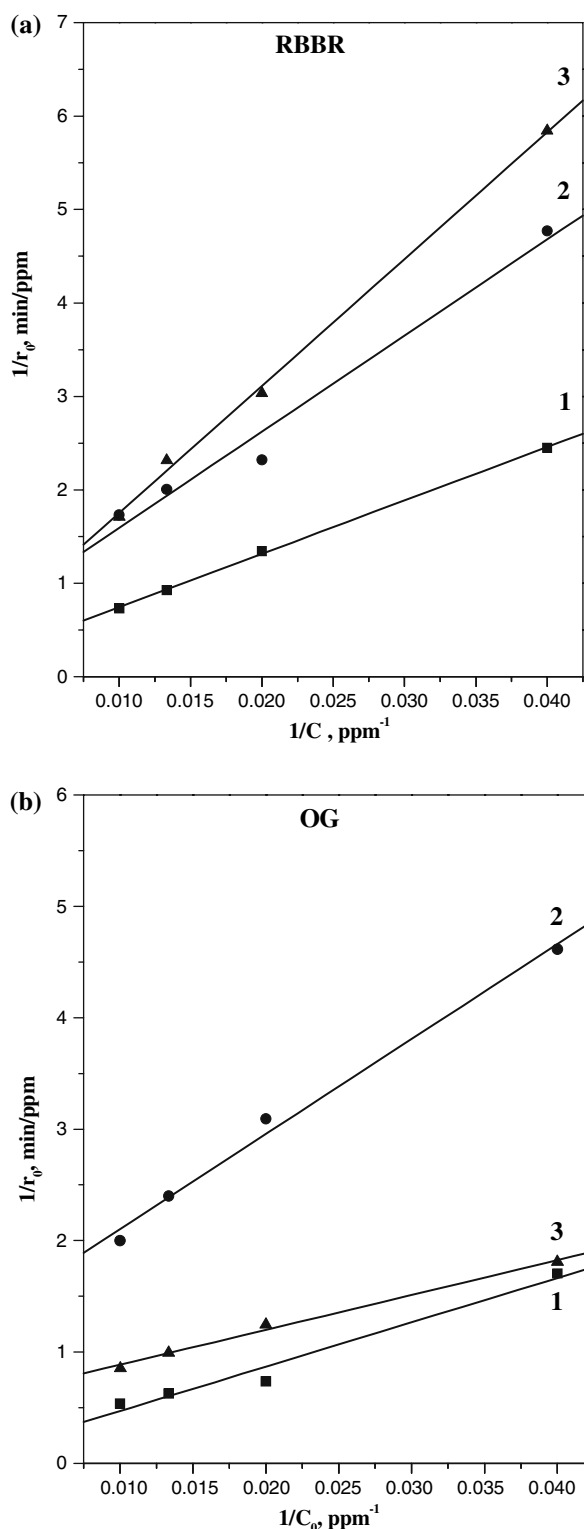
Figure 4. The variation of the initial photodegradation rate with the initial concentration of RBBR (a) and OG (b) by **1**, **2** and **3**.

Table 1
Kinetics parameters for the degradation of Dyes using $\{M(H_2O)_3\text{-}Co[C_5N_1H_3(COO)_2]_3\}$ M = Gd (**1**); Dy (**2**) and Y (**3**).

Compound	Dye	k_0 (min^{-1})	K_0 (ppm^{-1})
M = Gd (**1**)	RBBR	0.025	0.002
M = Gd (**1**)	OG	0.018	0.003
M = Dy (**2**)	RBBR	0.012	0.015
M = Dy (**2**)	OG	0.009	0.005
M = Y (**3**)	RBBR	0.032	0.018
M = Y (**3**)	OG	0.007	0.003

To conclude, the synthesis of a layered 3*d*–4*f* mixed-metal pyridine carboxylates of the general formula, $[M(H_2O)_3Co\{C_5N_1H_3(COO)_2\}_3])_\infty]$, M = Gd (**1**), Dy (**2**) and Y (**3**), has been accomplished. All the compounds are active for the photocatalytic decomposition of common organic dyes (RBBR and OG) used in textile industries, with activities better than commercial Degussa P-25 TiO$_2$. This study clearly reveals that it is profitable to investigate mixed-metal compounds as novel photocatalysts.

Acknowledgments

References

[1] J.M. Thomas and W.J. Thomas, *Principles and Practice of Heterogeneous Catalysis* (Wiley – VCH, Weinheim, 1996); M. Anpo and J.M. Thomas, Chem. Commun. (2006) 3273.

[2] J.M. Thomas, R. Raja and D.W. Lewis, Angew. Chem. Int. Ed. 44 (2005) 6445.

[3] M.R. Hoffmann, S.T. Martin, W. Choi and D.W. Bahnemann, Chem. Rev. 95 (1995) 69.

[4] D.S. Bhatkhande, V.G. Pangarkar and A.A. Beenackers, J. Chem. Technol. Biotechnol. 77 (2001) 102.

[5] A. Fujishima and K. Honda, Nature 238 (1972) 37.

[6] M. Hara, J.T. Lean and T.E. Mallouk, Chem. Mater. 13 (2001) 4668.

[7] O. Khaselev and J.A. Turner, Science 280 (1998) 425.

[8] M. Hara and T.E. Mallouk, Chem. Commun. (2000) 1903.

[9] Z. Zou, J. Ye, K. Sayama and H. Arakawa, Nature 414 (2001) 625.

[10] E. Papaconstantinou, Chem. Soc. Rev. 18 (1989) 1.

[11] G.B. Saupe, T.E. Mallouk, W. Kim and R.H. Schmehl, J. Phys. Chem. B. 101 (1997) 2508.

[12] G. Sivalingam, K. Nagaveni, M.S. Hegde and G. Madras, Appl. Catal. B 45 (2003) 23.

[13] Z.T. Yu, Z.L. Liao, Y.S. Jiang, G.H. Li, G.D. Li and J.S. Chen, Chem. Commun. 1814 (2004).

[14] Z.T. Yu, Z.L. Liao, Y.S. Jiang, G.H. Li and J.S. Chen, Chem. Eur. J. 11 (2005) 2642.

[15] D.S. Shephard, T. Maschmeyer, B.F.G. Johnson, J.M. Thomas, G. Sankar, D. Ozkaya, W.Z. Zhou and R.D. Oldroyd, Angew. Chem. Int. Ed. 36 (1997) 2242.

[16] J.M. Thomas, B.F.G. Johnson, R. Raja, G. Sankar and P.A. Midgley, Acc. Chem. Res. 36 (2003) 20.

compounds [14]. The observed differences in the activities for the photocatalytic degradation of the two dyes, among the three isostructural compounds, may be due to the differences in the efficiency of the electron transfer process from the organic dyes to the carboxylate radical.

[17] P. Mahata, G. Sankar, G. Madras and S. Natarajan, Chem. Commun. (2005) 5787.

[18] J. Huheey, E.A. Keiter and R.L. Keiter, *Inorganic Chemistry: Principles of Structure and Reactivity*, 4th edn., (Pearson Education, 2000).

[19] A.B.P. Lever, *Inorganic Electronic Spectroscopy* (Elsevier Publishing Company, 1968).

[20] J.B. Goodenough, *Magnetism and the Chemical Bond* (Interscience Publishers, 1966).

[21] M.B. Fleisher, K.C. Waterman, N.J. Turro and J.K. Barton, Inorg. Chem. 25 (1986) 3549.

[22] S. Moghaddas, P. Hendry, R.J. Geue, C. Qin, A.M.T. Bygott, A.M. Sargeson and N.E. Dixon, J. Chem. Soc., Dalton Trans. (2000) 2085.

[23] J.K. Barton and A.L. Raphael, J. Am. Chem. Soc. 106 (1984) 2466.

[24] C.H. Chang and C.F. Meares, Biochemistry. 23 (1984) 2268.

[25] C.H. Chang and C.F. Meares, Biochemistry. 21 (1982) 6332.

[26] F.A. Cotton, G. Wilkinson, C.A. Murillo and M. Bachmann, *Advanced Inorganic Chemistry* (John Wiley & Sons, Inc., NY, 1999).